◆ Human Brain Mapping 29:671–682 (2008) ◆

Low Frequency BOLD Fluctuations During Resting Wakefulness and Light Sleep: A Simultaneous EEG-fMRI Study

Silvina G. Horovitz,[1] Masaki Fukunaga,[1] Jacco A. de Zwart,[1] Peter van Gelderen,[1] Susan C. Fulton,[1] Thomas J. Balkin,[2] and Jeff H. Duyn[1]

[1]*Advanced MRI Section, LFMI, NINDS, National Institutes of Health, Bethesda, Maryland*
[2]*Department of Behavioral Biology, Walter Reed Army Institute of Research, Silver Spring, Maryland*

Abstract: Recent blood oxygenation level dependent functional MRI (BOLD fMRI) studies of the human brain have shown that in the absence of external stimuli, activity persists in the form of distinct patterns of temporally correlated signal fluctuations. In this work, we investigated the spontaneous BOLD signal fluctuations during states of reduced consciousness such as drowsiness and sleep. For this purpose, we performed BOLD fMRI on normal subjects during varying levels of consciousness, from resting wakefulness to light (non-slow wave) sleep. Depth of sleep was determined based on concurrently acquired EEG data. During light sleep, significant increases in the fluctuation level of the BOLD signal were observed in several cortical areas, among which visual cortex was the most significant. Correlations among brain regions involved with the default-mode network persisted during light sleep. These results suggest that activity in areas such as the default-mode network and primary sensory cortex, as measured from BOLD fMRI fluctuations, does not require a level of consciousness typical of wakefulness. *Hum Brain Mapp 29:671–682, 2008.*

Key words: fMRI; EEG; sleep; resting state; functional connectivity; low frequency fluctuations; default-mode network; visual cortex

INTRODUCTION

Sensory perception, motor activity, and cognition involve electrical and chemical signaling in many of the brain's cellular networks. The hemodynamic processes associated with this activity can be detected with positron emission tomography (PET) [Fox and Mintun, 1989; Mintun et al., 1984; Sadato et al., 1996] or blood-oxygen level dependent functional magnetic resonance imaging (BOLD fMRI) [Bandettini et al., 1992; Kwong et al., 1992; Ogawa et al., 1990]. These neuroimaging techniques were first used to study activity in brain networks by contrasting their signals during a sensory, motor, or cognitive task with those during a resting state, characterized by the absence of external stimuli. Implicit in this strategy is the assumption that there is an invariantly low level of neuronal activity in the resting state.

This article contains supplementary material available via the Internet at http://www.interscience.wiley.com/jpages/1065-9471/suppmat

Material has been reviewed by the Walter Reed Army Institute of Research. There is no objection to its presentation and/or publication. The opinions or assertions contained herein are the private views of the author, and are not to be construed as official, or as reflecting true views of the Department of the Army or the Department of Defense.

This research was funded by National Institute of Neurological Disorders and Stroke (NINDS) Intramural Program.

*Correspondence to: Silvina G. Horovitz PhD, 9000 Rockville Pike, Building 10, Room B1D722, Bethesda, MD 20814-1065, USA.
E-mail: silvina.horovitz@nih.gov

Received for publication 7 December 2006; Revised 13 April 2007; Accepted 26 April 2007

DOI: 10.1002/hbm.20428
Published online 27 June 2007 in Wiley InterScience (www.interscience.wiley.com).

However, during resting wakefulness, a substantial level of electrical and metabolic brain activity exists. In the EEG, the presence of a regular 'idling' rhythm was observed in scalp voltage as early as the 1920s which, somewhat paradoxically *decreased* in amplitude when subjects opened their eyes or became more engaged in a task [Berger, 1929]. Slower and more irregular fluctuations were also clearly observable in resting animals, and appear to be controlled as much by brainstem centers as by sensory stimulation [Moruzzi and Magoun, 1995]. Moreover, many individual neurons show a high spontaneous firing rate that is not significantly attenuated even when an animal falls into sleep [Evarts et al., 1962].

The influence of the ongoing EEG activity in cortical function and cognitive processes has recently received new interest following a set of studies by Arieli et al., in the 1990s [Arieli et al., 1996; Creutzfeldt et al., 1966], with recent work suggesting that large spontaneous activity fluctuations commonly occur over time scales that match the dynamics of resting state BOLD fluctuations [Leopold et al., 2003]. Most interestingly, evidence suggests that the ongoing rhythms contribute to the majority of the brain electrical activity and the evoked/event-related activity, if present, contributes to only a small percentage of the variance [Raichle, 2006].

In a meta-analysis of PET studies, Shulman et al. [1997a] showed two distinctive hemodynamic behaviors. Based on data from nine studies, it was shown that visual tasks consistently result in blood flow changes confined to visual cortex. When subjects performed tasks that were cognitively more demanding, a set of deactivated areas was observed [Shulman et al., 1997b] together with the activated cognitive areas. These findings led to the study of the so-called "default-mode network" [Raichle et al., 2001], defined as the network of brain regions that become more active when goal-directed cognitive activity ceases. This network has been hypothesized to facilitate functions such as the monitoring of the body and environment, maintenance of consciousness, and ongoing conscious processes including internal information retrieval, and cognitive information processing [Binder et al., 1999; Mazoyer et al., 2001; McGuire et al., 1996]. The default-mode network includes dorsal medial prefrontal cortex, posterior cingulate, precuneus, and inferior parietal cortex.

In BOLD fMRI studies, temporally correlated signal fluctuations have been observed during the resting state in distinct regions including sensory areas [Biswal et al., 1995; Cordes et al., 2000, 2001; Lowe et al., 2000], language areas [Hampson et al., 2002], as well as the default-mode network [Greicius et al., 2003]. The temporal frequencies present in these fluctuations are concentrated in the 0.005–0.05 Hz range [Cordes et al., 2001; Fransson, 2006; Fukunaga et al., 2006]. Using independent component analysis (ICA) of resting state data, it has been shown that many networks exist with apparent functional significance, and with spatial distributions and signal time courses that are largely independent [De Luca et al., 2006; Fukunaga et al., 2006].

The origin and role of these BOLD fMRI fluctuations, usually referred to as resting state activity, remain unknown. Although they may, in part, reflect purely vascular processes [Mitra et al., 1997] and may partly relate to systemic fluctuations linked to arterial CO_2-induced changes in cerebral blood flow [Wise et al., 2004], hemodynamic fluctuations in fMRI, near infrared spectroscopy (NIRS) and PET have been shown to correlate with underlying electroencephalographic activity [Goldman et al., 2002; Laufs et al., 2003; Moosmann et al., 2003; Obrig et al., 2000; Sadato et al., 1998]. Furthermore, the multiple fine-scale, temporally independent, and reproducible patterns of fluctuations found in the ICA studies of fMRI data [Arfanakis et al., 2000; De Luca et al., 2006; Fukunaga et al., 2006; van de Ven et al., 2004] suggest these fluctuations are not systemic and have functional relevance.

To the extent that resting state BOLD fMRI activity relates to brain function, is it representative of a conscious waking state[1]? Does it depend on the level of consciousness? Preliminary studies of resting state BOLD activity during conditions of reduced consciousness, such as sleep [Fukunaga et al., 2006] and sedation [Kiviniemi et al., 2005] found continued resting state activity in widespread brain regions, including sensory areas such as visual cortex. This suggests that BOLD resting state fluctuations in these regions do not require conscious activity. Here, we extend our previous study [Fukunaga et al., 2006] by adding simultaneous EEG recordings to allow direct correlation of the resting state BOLD fMRI fluctuation levels (see below) with the level of consciousness, as reflected by polysomnography. Furthermore, in the present study, we aimed at establishing whether correlated BOLD signal fluctuations in the default-mode network persist at the reduced levels of consciousness characteristic of light sleep.

METHODS

Experimental Design

The paradigm used by Fukunaga et al. [2006] was modified to extend the time available for subjects to sleep. Our 60-min paradigm (Fig. 1) started with a 1-minute long period of quiet wakefulness with eyes open, after which the subjects were instructed to close their eyes, relax and try to sleep. Subjects were allowed to sleep undisturbed for 48 min, after which they were instructed to open their eyes. Starting from minute 50, a flickering checkerboard (6 Hz) was presented, stimulating alternately the central 5° of the visual field or its periphery (5°–15°), in seven blocks of 48 s each. During the last 4.4 min, the volunteers were

[1]Throughout this work, we equate consciousness to the waking state [Zeman, 2001]. Defined this way, consciousness is a matter of degree that extends from waking through sleep into anesthesia and coma [see also Laureys, 2005].

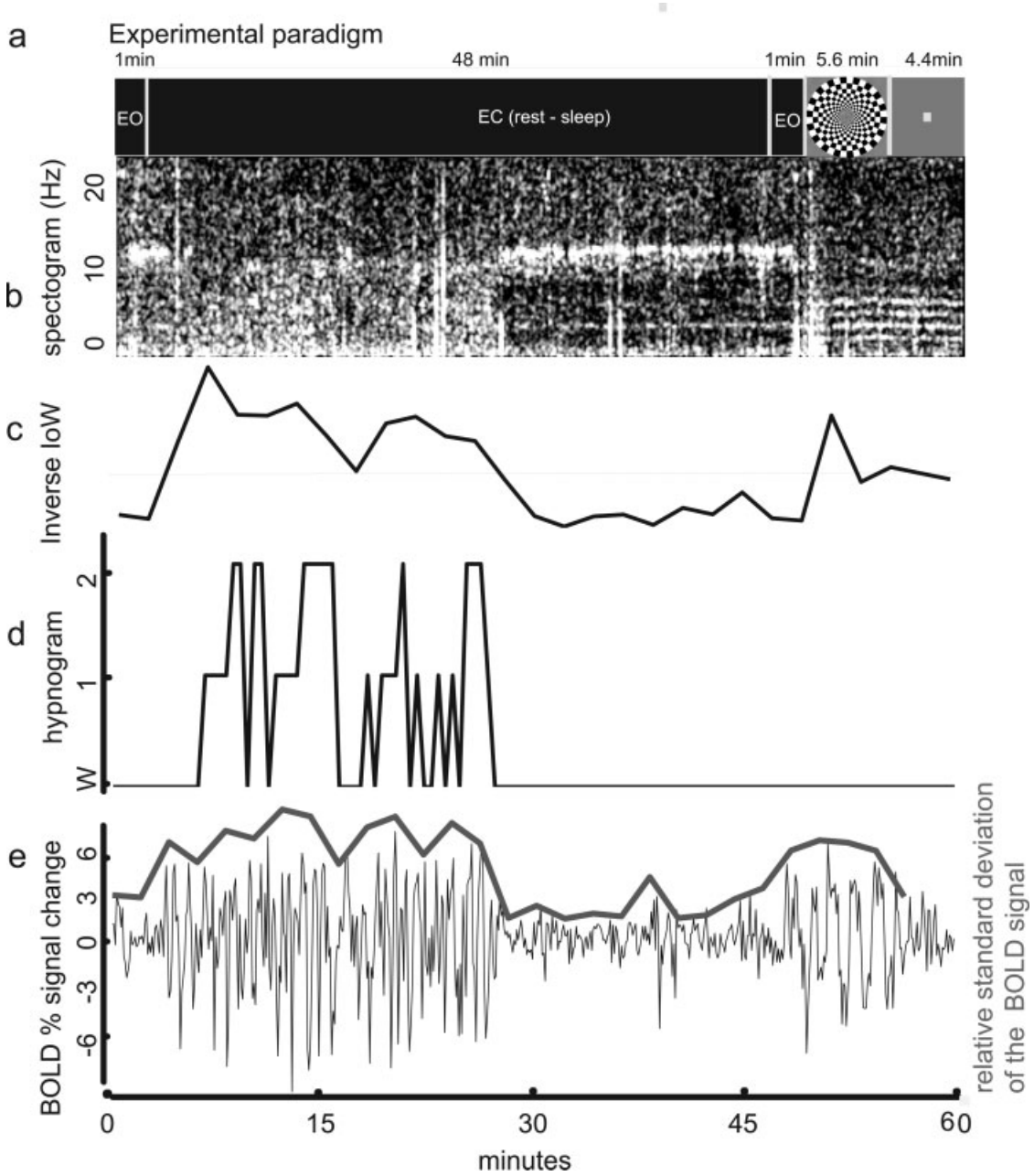

Figure 1.

Experimental paradigm and sample time course data from one subject. (**a**) Timing of the scan paradigm. One minute of rest with eyes open (EO) was followed by 48 min of eyes closed (EC), during which the subject was allowed to sleep. This was followed by another minute of EO, and 5.6 min of checkerboard stimulation and 4.4 min of center dot fixation for a total scan time of 60 min. (**b**) EEG spectrogram: time-frequency spectrum of the data from one subject at electrode C3. Notice elevated alpha activity (8–12 Hz) -indicating *wakefulness*- at the beginning, then slowing towards extended theta (2–7 Hz) - indicating *sleep*- and just before minute 30 returning to predominantly alpha activity. (**c**) Inverse index of wakefulness (IIoW): Larger values represent lower frequencies in the EEG, which are associated with sleep. (**d**) Hypnogram: Sleep score, over 30 s intervals, as assessed by sleep expert (TJB). Higher scores indicate deeper sleep (Rechtschaffen and Kales, 1968). (**e**) fMRI time course: average percentage signal change in the VC ROI, defined from the response to the visual task. Overlay: relative standard deviation of the BOLD signal change in the VC ROI, in 2 min (20 images) intervals, data offset vertically by 3 units for display purposes.

instructed to fixate on a dot in the center of the visual display.

Simultaneous EEG and fMRI data were collected in twenty two sessions from fourteen subjects (5 females, 9 males; age range: 21–56, average age: 32) after each provided written informed consent in accordance with a protocol approved by the National Institutes of Health (NIH) Intramural Research Board (IRB). Ear-plugs were inserted for hearing protection. All studies were performed during the daytime. All subjects reported normal sleep/wake patterns, and no prior sleep deprivation or any other manipulation was performed to facilitate sleep onset in the scanner.

Physiological Recordings

EEG was collected using silver-silver chloride sintered electrode caps via carbon fibers (MagLink) using Synamps2 amplifiers and Scan 4.3 software (all from Neuroscan, Compumedics USA Ltd, El Paso, TX). Forty electrodes, including those in the standard 10–20 International system, were used. The ground electrode was located frontal to Fz and the reference electrode was between Cz and Pz, all on the brain midline. Two bipolar electrodes were used to monitor electro-oculogram (EOG) and cardiac signal (ECG). Acquisition rate was 10 kHz, with a low pass filter set to 3 kHz. Data were collected continuously. Respiration was measured using respiratory bellows and cardiac rate was measured using a pulse oximeter placed on the left index finger. Both transducers were provided with the MRI scanner. Signals from respiratory and cardiac sensors and scanner-generated TTL trigger pulses were collected at a frequency of 1 kHz to allow adequate sampling of the cardiac signal [Lund et al., 2006].

fMRI Data Acquisition

BOLD fMRI was acquired on a 3T scanner (GE Signa, Milwaukee, WI) using a 16-channel receive-only detector array (Nova Medical, Wakefield, MA) [de Zwart et al., 2004]. The coil was foam-padded to restrict head motion and improve subject comfort. After a 3D localizer, single-shot echo-planar-images (EPI) were collected from 28 oblique-axial slices (1.7×1.7 mm^2 nominal in-plane resolution, 3.0-mm thickness, 0.5-mm gap) covering most of the brain. Cerebellum and subthalamic nuclei were often only partially included. The excitation flip angle was set to 90°. Repetition time (TR) was 6 s and echo time (TE) was 43 ms. The MRI slice acquisition was grouped (bunched) in time in the first 3 s of the TR to allow for 3 s of EEG without contamination from gradient artifacts. A TR of 6 s is longer than typically used, but it should capture most of the low frequency BOLD signal fluctuations with only little contribution of aliased cardiac and respiratory signals [see frequency distribution in Fukunaga et al., 2006]. 3D T_1-weighted images were collected from all volunteers using a GE head-coil in a different session, using an IR-prepared 3D SPGR sequence (MPRAGE).

Data Analysis

Data analysis was performed to characterize resting state activity during both wakefulness and sleep. EEG data was scored using Rechtschaffen and Kales [1968] criteria to determine sleep stage, and further processed to derive an index of wakefulness as described below. Subsequently, fMRI data was analyzed to determine the relationship between this index and the fluctuation level, and to investigate resting state correlations and fluctuation levels of the BOLD signal during both waking rest and light sleep. For this purpose, whole brain analysis was performed, as well as more focused analyses in selected ROIs, as defined below.

EEG Pre-Processing

After low-pass filtering at 250 Hz, artifacts induced by MRI gradient switching were removed based on template subtraction [Allen et al., 2000]. Subsequently, band-pass filtering was performed using a frequency range of 0.5–28 Hz. Cardio-ballistic artifact was removed by first detecting the R-wave and creating an averaged template of the artifact, then extracting its principal components and finally removing those components from the original data. All these procedures were performed using Scan 4.3.2 software (Neuroscan, Compumedics USA Ltd, El Paso, TX).

Determination of Sleep Stage and Index of Wakefulness

EEG datasets were visually inspected by a sleep expert (TJB). A sleep stage (wakefulness (W), Stage 1, Stage 2, slow wave sleep (SWS) or rapid eye movement (REM)) was generated for each 30-s interval. Frequency analysis was performed using IDL 6.2 (ITT visual information solutions, Boulder, CO, USA) for electrodes C3, C4, P3, and P4. EEG of wakefulness while resting with eyes closed is characterized by a relatively high level of α activity (8–12 Hz), while lower frequencies are more prominent during non-REM (NREM) sleep [Rechtschaffen and Kales 1968]. Therefore, wakefulness was quantified by taking the ratio of the square root of the power in the 2–7 Hz band to that in the alpha band, computed over 2-min intervals. In the present article, we refer to this value as the inverse index of wakefulness (IIoW), since a higher index corresponds to a lower waking consciousness level. We compared the IIoW to the fluctuation level of the fMRI percentage signal change as described below.

fMRI Preprocessing

Data sets were processed using custom routines written in IDL, unless otherwise specified. First, each run was registered to the last image in the time series. Slice timing correction and rigid body motion correction were performed using SPM2 software (Wellcome Department of Cognitive

Neurology, London, UK). The following procedures were performed on the "resting state" data (min 1–49): A high-pass filter (0.006 Hz) was applied to remove baseline drift. The global signal change was removed by linear regression of the time course of the average brain signal, after brain/skull segmentation [Birn et al., 2006; Fukunaga et al., 2006]. The cardiac rate and the respiratory depth, derived from the peak to peak amplitude of the respiratory trace [Birn et al., 2006]—were also regressed out. The cardiac rate and respiration regressors were estimated by correlating the physiological signals with the fMRI BOLD signal for each voxel at different delays (±10 TRs), then averaging the correlation coefficient across whole brain for each delay and finally selecting the delay with highest correlation (typically 1 or 2 TRs). Images were registered to a standard MNI brain ($2 \times 2 \times 2$ mm^3). Data sets were converted to percentage signal change by subtracting the mean value of each voxel from its time course, then dividing by the mean and multiplying by 100.

ROI Definitions

In addition to whole brain analysis of the fluctuation levels, several analyses were also performed on predefined regions of interest. A visual cortex (VC) ROI was defined functionally for each subject by selecting the voxels in the occipital region that correlated significantly ($r > 0.5$) with the central visual stimulation paradigm. The average time course of this ROI was used as the seed for the VC correlation analysis (see below).

ROIs in posterior cingulate, precuneus, anterior cingulate, superior occipital, calcarine sulcus, supplementary motor area, inferior parietal, and inferior frontal gyri were chosen to explore the default-mode network and the areas that (anti) correlate with it, sensory processing and attention areas. These ROIs were prescribed from a MNI template [Tzourio-Mazoyer et al., 2002], since no task was performed for their definition (details about the ROIs are shown in supplementary information: Figs. S1 and Table SI). The average time course of the posterior cingulate ROI was used as the seed for the default-mode network correlation analysis (see below). The posterior cingulate ROI time course was correlated with the time course of a seed selected using coordinates from Raichle's work (Talairach −5, −49, 40) [Raichle et al., 2001].

Fluctuation Level of the BOLD Signal as a Function of the Inverse Index of Wakefulness

After fMRI pre-processing, the fluctuation level of the BOLD signal was estimated for each voxel in the brain from the standard deviation of the BOLD signal and expressed as percentage. For a zero mean signal, the standard deviation approximates the root mean square (r.m.s) of the fluctuation level, a measure of the amount of energy in the signal fluctuation.

TABLE I. BOLD fluctuation differences between wakefulness and sleep in the VC ROI

	VC ROI		
Subject	Wakefulness	Sleep	Task
s1	1.42	1.51	2.91
s2	1.63	1.74	1.95
s3	1.42	1.89	1.58
s4	1.11	1.16	1.42
s5	1.21	1.26	1.84
s6	1.33	1.48	1.03
s7	1.27	1.28	1.00
s8	1.23	1.33	1.65
s9	1.68	1.84	1.95
s10	1.08	1.06	1.19
s11	1.45	1.76	1.71
Mean (±s.d)	1.35 (± 0.19)	1.48 (± 0.29)	1.65 (± 0.53)
Wilcoxon test (*P*-value)	0.0029		

The fluctuation level of the BOLD signal, expressed as relative standard deviation, was computed for each voxel and averaged within the ROI (see methods). Values during task are also presented for comparison.

To allow sufficient accuracy for the determination of the fluctuation level of the BOLD signal, only subjects that had a minimum of two uninterrupted minutes each of sleep and wakefulness were included in this analysis. The fluctuation level was calculated for each 2-min interval during the resting part of the experiment as indicated above, for each voxel after smoothing using a 2-pixel Gaussian filter. The length (2 min) of the intervals was chosen to have enough time points for the level estimation (20 TRs) but also enough points for the regression (22 two-minute intervals). For each voxel in the brain, the fluctuation level was correlated to the IIoW computed over the same 2-min intervals. Significance was established by permutation methods [Holmes et al., 1996].

For the VC ROI, the same analysis was repeated without Gaussian filtering. Data from the VC ROI were further explored by combining the fluctuation level of all voxels within the ROI for each condition (wakefulness or sleep) and compared using Wilcoxon's test. Measures during the visual task are reported as a comparison.

We computed the power spectral density of the BOLD signal over the VC ROI to allow comparison with previous studies [Fransson, 2006; Fukunaga et al., 2006].

Temporal Correlation During Sleep and Wakefulness

To allow sufficient accuracy for determination of temporal correlation, only subjects who had a minimum of 45 contiguous time points (4.5 min) each of sleep and wakefulness were included in this analysis. Functional connectivity was computed as the correlation of the seed time courses with all other voxel time courses. The reference time course (seed) was created by averaging the time

course signals of all voxels belonging to the selected ROI (VC or Posterior Cingulate). All preprocessing was performed prior to this analysis, as indicated in *fMRI Preprocessing* section.

Spatial Extent of Correlated Activity in the Default-Mode Network and Visual Cortex

The spatial extent of the temporal correlation in default-mode network and visual cortex was determined by correlation with the time course of the posterior cingulate seed region and the functional VC time course, respectively. This was done in both sleep and wakefulness. Correlation coefficients were converted to *z*-scores using Fisher's transformation [Howell, 1997] to account for individual variability [Hampson et al., 2002] and combined across subjects. Significance level (*P*-value) was established by a randomization method in which phase data was scrambled [Bullmore et al., 1999].

Strength of the Correlation of the fMRI Signal Within ROIs

The strength of the correlation within each ROI was computed separately for sleep and wakefulness by correlating the voxel-averaged time course of each ROI with time courses of the individual voxels in that ROI. The resulting correlation values were then averaged, and a *t*-test was performed to determined significance of differences between sleep and wake conditions.

RESULTS

Data Quality and Subject Inclusion

Despite the adverse conditions of MRI scanning (gradient acoustic noise, fixed head and body position), most subjects were able to fall asleep during at least one of the sessions, displaying mostly light sleep. In all but one subject no deep sleep was observed, which is attributed to the nonsleep-conducive experimental conditions, and the fact that scans were performed during daytime hours without prior sleep deprivation.

For sixteen of the twenty two-data sets, the EEG data was of sufficient quality to discriminate between sleep and wakefulness, both by IIoW and by sleep scoring done by the sleep expert (TJB). The six remaining data sets were excluded from further analysis either due to apparent motion artifacts (5 mm or more in estimation of the motion correction during the image registration procedure) or due to incomplete data sets resulting from technical problems.

Three data sets did not include any sleep. Thirteen of the sixteen data sets had at least 2 min of wakefulness and 2 min of sleep. They were collected from eleven subjects, so two more studies were excluded to have only one data set per subject. Those data sets that presented more continuous segments of sleep and wakefulness were included in the analyses.

For the eleven subjects included in this study, the mean sleep efficiency index, defined as the percentage of time scored as sleep over the total time allowed for sleep, was 22.28%, ranging from 2.0 to 23.0 min. Most of the sleep data were scored as Stages 1 and 2, with only one subject reaching SWS for 2 min.

Only six subjects had more than 4.5 consecutive minutes of sleep and more than 4.5 consecutive minutes of wakefulness, and were thus included in the temporal correlation analysis. For these six subjects, the average time included in the analysis for each condition was 12.6 ± 2.6 min.

Consistent with an earlier report from our laboratory [Fukunaga et al., 2006], the 11 subjects included in this study showed, during the 48-min "eyes-closed" portion of the study, an fMRI signal fluctuation level in grey matter[2] (1.14% of the baseline signal intensity) that was substantially above thermal noise level[3] [de Zwart et al., 2002] (0.44% of the baseline signal intensity) and that was comparable to the signal changes during task performance (Table I and Fig. 3a).

Fluctuation Level of the BOLD Signal as a Function of the Inverse Index of Wakefulness

This analysis was performed on the 11 subjects matching the "2 min sleep and 2 min wakefulness" criterion. The power spectral density is shown in Figure 2. Most of the energy was concentrated below 0.03 Hz, and some expanding to 0.05 Hz, similar to the range observed in previous work [Fransson, 2006; Fukunaga et al., 2006].

The BOLD signal fluctuation level observed in the VC during sleep periods was larger than during resting wakefulness and was generally comparable to the amplitude of activation evident during the performance of the visual task (see example in Figs. 1 and 3a). Correlation of the fluctuation level with IIoW and comparison with sleep scoring showed that, as subjects fell asleep, the BOLD fluctuation level in the VC generally increased (Fig. 3b and Table I). The correlation between the relative standard deviation of the BOLD signal in the VC and the IIoW reached $r = 0.37$ ($F_{(11,223)} = 12.139$, $P < 0.025$) (Fig. 3b).

The whole brain maps were surface rendered with SUMA [Saad et al., 2006] for display purposes. Areas that showed fluctuation levels significantly correlated to the IIoW are shown in Figure 3c. As subjects fall asleep, an increase in fluctuation level is seen in widespread cortical regions, especially in the sensory areas (different parts of visual, motor and primary auditory cortices), in precuneus, and to a lesser extent in inferior parietal, supramarginal,

[2]Signal was computed from an ROI defined as the sum of all grey matter areas from an MNI template [Tzourio-Mazoyer et al., 2002].
[3]Thermal noise is random noise that can be calculated from an EPI acquisition without RF excitation [de Zwart, 2002].

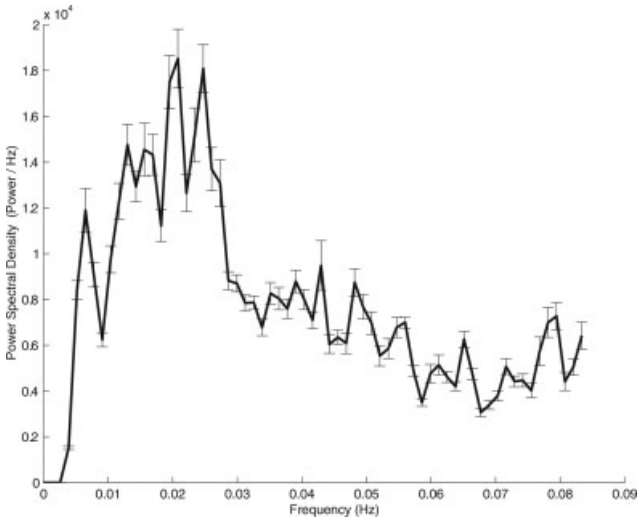

Figure 2.
Power spectral density of the BOLD time course in the VC ROI computed for 11 subjects over the entire (48 min) resting period.

and temporal cortices as well as in parts of frontal gyri, paracentral areas, and also in some deep structures as thalamus, caudate, and putamen. Decreases were seen in the medial frontal gyri, although they did not reach significance.

In the VC ROI the fluctuation level of the BOLD signal was significantly larger ($P < 0.0029$) during sleep compared to wakefulness (data reported in Table I).

Temporal Correlations During Sleep and Wakefulness

This analysis was performed in the six subjects who obtained at least 4.5 uninterrupted min of both sleep and wakefulness.

Analysis of the temporal correlation with the average time course in the VC showed a similar spatial pattern during both sleep and wakefulness (Fig. 4). Figure 5 shows the composite maps for wakefulness and sleep detected by correlation with the average time course in the posterior cingulate.

The default-mode network was present both during wakefulness and light sleep and had a similar spatial extent during these conditions. It was also detected during both conditions in each of the individual subjects (data shown in supplementary Fig. S2). The correlation between the averaged ROI time course and the time course of the seed reported by Raichle et al. [2001] was significant ($r = 0.46$) and the correlation maps using that seed provide similar results (supplementary Fig. S3). The nonoverlapping spatial distribution of the networks detected by correlation with VC and posterior cingulate seeds suggest these represent two independent processes present in the resting state (supplementary Fig. S4).

Within-ROI correlation coefficient values were significant for all ROIs, and similar for light sleep and wakefulness for most of the defined areas (Table II). Significantly larger coefficients during sleep were seen bilaterally in supplementary motor area ($t > 2.5$, $P < 0.0272$) and in right calcarine sulcus ($t = 2.13$, $P = 0.043$). None of the selected areas showed larger correlations during wakefulness compared to sleep. These results indicate that significant functional connectivity within the selected ROIs is present during both sleep and wakefulness.

DISCUSSION

General Remarks

In this work, EEG and fMRI were performed simultaneously to study the effect of sleep on resting state BOLD activity throughout the brain. Collecting simultaneous EEG/fMRI sleep data in the scanner during daytime hours without any sleep deprivation proved challenging. While most volunteers slept fitfully for parts of the study, only a modest number (six) slept uninterrupted for at least 4.5 min, limiting the amount of data available for the analyses involving correlations. However, results were obtained both at individual subject and group level. The use of a relatively long TR of 6 s provided results similar to our previous data collected at 3 s TR, and the spectral distribution was similar to that reported previously [Fransson, 2006; Fukunaga et al., 2006] suggesting a minimal contribution of aliased cardiac and respiratory signals in the present results [see also Lowe et al., 1998].

Presence of Resting State Activity During Sleep

Consistent with a preliminary earlier report from our laboratory [Fukunaga et al., 2006], widespread fMRI resting state activity was observed during sleep. This was evident from both fluctuation levels and temporal correlation analysis. It is intriguing that some areas, including primary visual cortex, showed an increase in resting state fluctuation levels with sleep and reduced levels of consciousness. The continued presence of correlated fluctuations during sleep suggests that BOLD fMRI resting state activity does not require conscious wakefulness but rather, in most brain areas, persists during the reduced levels of consciousness characteristic of light sleep. This notion of a continuation of resting state activity with reduced consciousness is consistent with a previous study that found and increase in BOLD fMRI signal correlation in visual cortex after sedation [Kiviniemi et al., 2005]. The fluctuation level increases found in selected brain regions with sleep and sedation are intriguing and require further investigation.

Another important finding of the current study is the continued presence of correlated BOLD signal fluctuations in the default-mode network during light sleep. This new finding suggests that the default-mode network is active

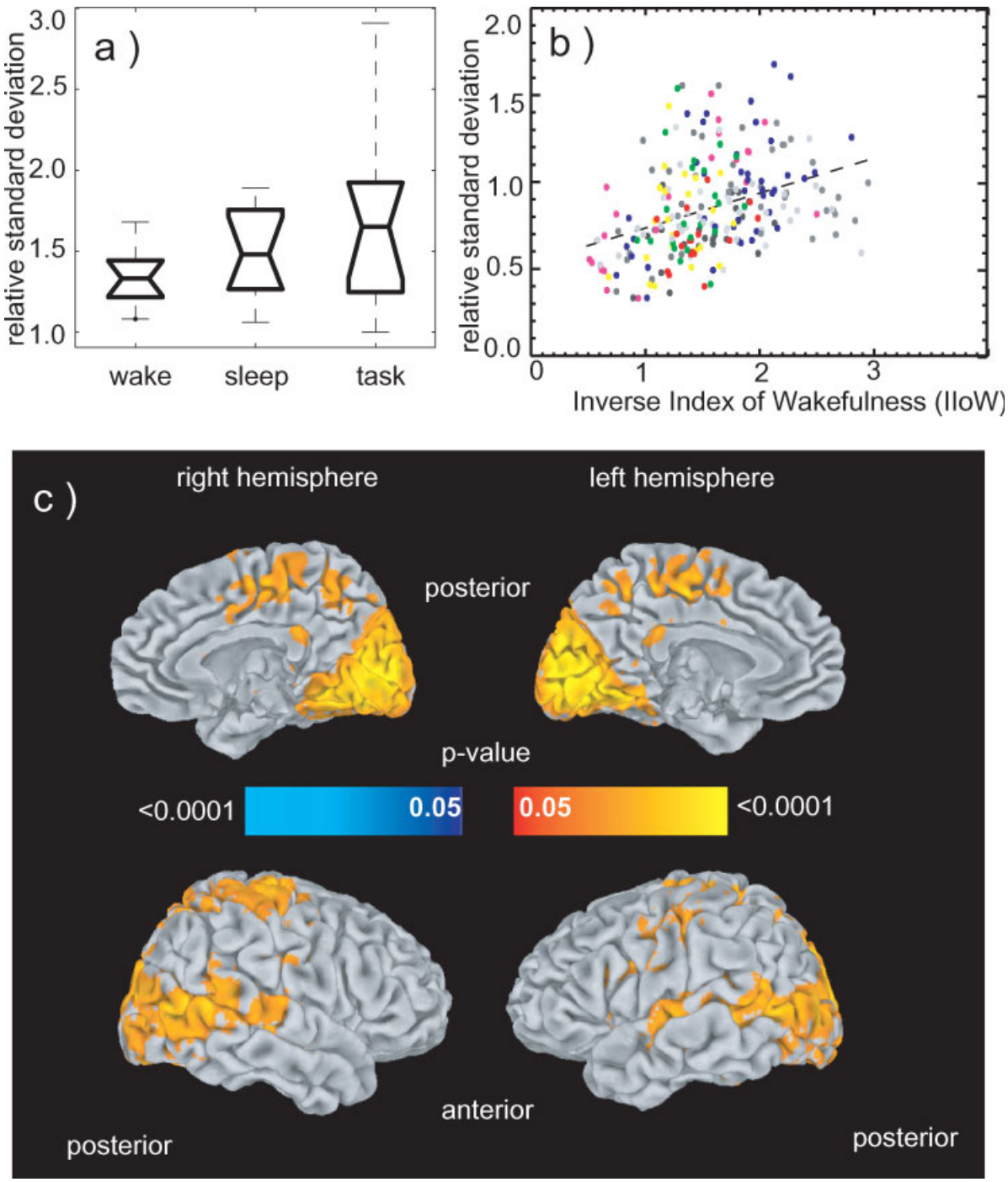

Figure 3.

BOLD fluctuation differences between sleep and wakefulness (n = 11). (**a**) Boxplot of the relative BOLD signal fluctuation levels in VC during resting wakefulness, sleep and task. The boxes have lines at the lower quartile, median, and upper quartile values. The whiskers are lines extending from each end of the box to show the extent of the rest of the data. These data have no outliers. (**b**) Relationship between fluctuation level of the BOLD signal and IIoW in the visual cortex ROI. Scatter plot shows relative standard deviation of the BOLD percentage signal change averaged over the VC ROI, versus IIoW. Each point is obtained as an average over 2 min intervals (that is over 20 TRs). Two hundred and thirty-five points derived from eleven subjects are presented (22 intervals per subject, two subjects contributed 17 and 19 points respectively due to shorter scans). Each color represents a volunteer. The regression curve is shown by the dotted line. Correlation coefficient = 0.37, $F_{(11,223)} = 12.139$, $P < 0.025$). (**c**) Relationship between fluctuation level of the BOLD signal and IIoW across the entire brain. Correlations between relative standard deviation of the BOLD percentage signal change in each voxel and IIoW converted to p-values and shown on inflated brain. Yellow-red tones indicate areas where fluctuations are larger during sleep compared to wakefulness (larger IIoW). A widespread distribution of this effect is seen in visual cortex, primary auditory cortex, and precuneus among other areas. Blue tones (not seen) indicate areas where fluctuations during wakefulness were larger than during sleep.

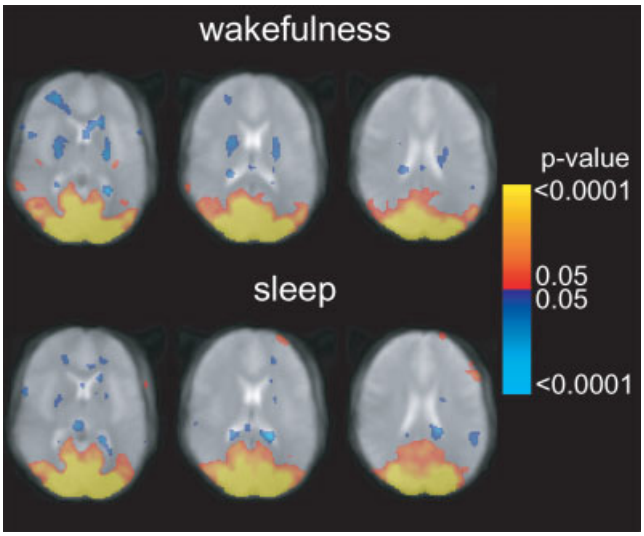

Figure 4.
Statistical composite maps (n = 6) showing the temporal correlation of the percentage BOLD signal change with the mean time course in the VC ROI during wakefulness (top) and sleep (bottom). Color scale represents p-values, thresholded at $P = \pm 0.05$ (corrected). Positive (red-yellow) and negative (blue) correlations are shown.

and functionally connected in the absence of goal-directed mental activity, not only during awake rest [Gusnard and Raichle, 2001; Raichle et al., 2001], but also during light sleep. This network has previously been hypothesized to subserve monitoring of the environment, conscious awareness, sustained information processing or retrieval, and manipulation of episodic memory [Greicius et al., 2003; Gusnard and Raichle, 2001; Raichle et al., 2001]. Furthermore, its activity has been shown to increase during brief periods of impaired performance after sleep deprivation [Drummond et al., 2005]. The observed connectivity within this network during sleep in the current study suggests that it does not require or reflect the level of consciousness that is typical of wakefulness.

Comparison With Previous Neuroimaging Studies

The results of the current study are based on analysis of signal fluctuation levels, and do not provide information about absolute BOLD signal at specific sleep stages. This was not attempted because absolute activity is difficult to extract reliably form BOLD signals. This makes it difficult to compare the current findings directly to many earlier PET neuroimaging studies of sleep, which report on steady state levels of cerebral blood flow (CBF) or glucose utilization PET [Andersson et al., 1998; Braun et al., 1997; Buchsbaum et al., 1984; Hofle et al., 1997; Kajimura et al., 1999, 2004; Kjaer et al., 2002; Maquet, 2000; Maquet et al., 1992; Nofzinger et al., 2002; Peigneux et al., 2001]. In general, these studies observed CBF and metabolism decreases during NREM sleep. However, only few of these studies have reported on differences between deep sleep (Stages 3 and 4) and light sleep (Stages 1 and 2) [Kjaer et al., 2002; Maquet et al., 1992]. Maquet et al. [1992] found non-significant changes in most areas, whereas Kjaer et al. [2002] found (during Stage 1) increases in extrastriate areas and decreases in posterior parietal cortex, cerebellum, premotor cortex and thalamus.

Similarly, comparison with previous EEG/fMRI studies that have investigated resting state activity is difficult as these studies did not look at BOLD fluctuation levels, as the current study did, but rather directly correlated EEG signals with BOLD signal levels. Additionally, level of wakefulness was not reported. In general, these studies found a negative correlation of BOLD signal with alpha power [Goldman et al., 2002; Laufs et al., 2003; Moosmann et al., 2003] in the visual cortex. Laufs et al. [2006] reported two distinctive networks correlating with alpha power and speculated that vigilance levels could affect the relative network activity. We find increases in signal fluctuations in the visual cortex and other cortical areas with increased levels of IIoW, suggesting that the vigilance level does indeed affect the resting BOLD signal fluctuations.

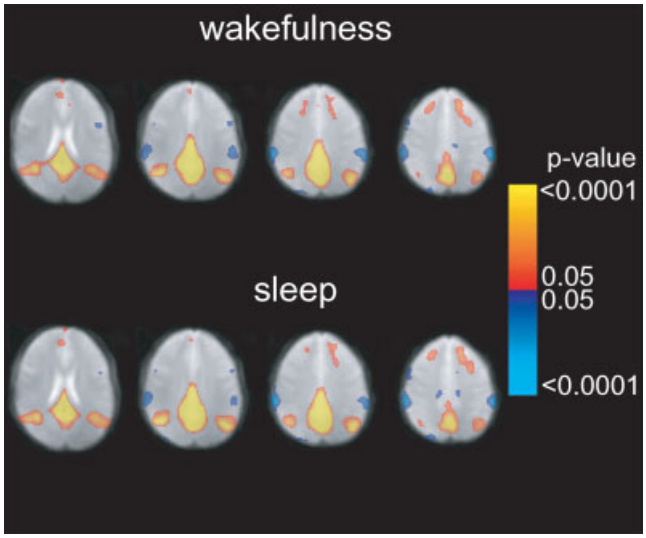

Figure 5.
Statistical composite maps (n = 6) showing the temporal correlation of the percentage BOLD signal change with the seed in the posterior cingulate ROI during wakefulness (top) and sleep (bottom). Four representative axial slices show similar default-mode network correlations during wakefulness and light sleep. Color scale represents p-values, thresholded at $P = \pm 0.05$ (corrected). Positive (red-yellow) and negative (blue) correlations are shown.

TABLE II. Strength of the within-region correlation during wakefulness and sleep

ROI	Hemisphere	T-T coordinates			No. of voxels ($2 \times 2 \times 2$ mm^3)	Average r (±s.d.)		z-score	
		x	y	z		Wakefulness	Sleep	Wakefulness	Sleep
Precuneus	L	6	−59	41	3,265	0.53 (±0.08)	0.52 (±0.04)	1.8	1.78
	R	−10	−59	37	3,528	0.45 (±0.07)#	0.46 (±0.04)	1.69	1.7
Posterior cingulate	L	4	−45	21	335	0.71 (±0.06)	0.72 (±0.08)	2.1	2.12
	R	−8	−44	18	463	0.62 (±0.07)	0.62 (±0.07)	1.93	1.93
Anterior cingulate	L	3	30	16	1,313	0.61 (±0.07)	0.61 (±0.08)	1.91	1.92
	R	−9	31	21	1,400	0.57 (±0.06)	0.60 (±0.03)	1.85	1.89
Superior occipital	L	15	−84	21	1,413	0.62 (±0.08)	0.65 (±0.05)	1.94	1.98
	R	−24	−81	24	1,366	0.60 (±0.06)	0.64 (±0.03)	1.9	1.95
Supplementary motor area	L*	4	−4	56	2,371	0.55 (±0.03)	0.60 (±0.04)	1.82	1.89
	R*	−9	−8	56	2,147	0.45 (±0.05)#	0.50 (±0.04)	1.68	1.75
Inferior parietal	L	40	−49	40	1,345	0.59 (±0.06)	0.58 (±0.05)	1.88	1.86
	R	−44	−50	42	2,447	0.60 (±0.06)	0.60 (±0.05)	1.9	1.9
Inferior frontal	L	42	23	15	2,151	0.54 (±0.05)	0.57 (±0.03)	1.8	1.86
	R	−48	23	16	2,529	0.53 (±0.05)	0.55 (±0.06)	1.79	1.82
Calcarine sulcus	L	6	−77	2	1,861	0.67 (±0.07)	0.71 (±0.04)	2.03	2.09
	R*	−16	−72	5	2,258	0.54 (±0.09)	0.61 (±0.08)	1.81	1.91

Mean r and standard deviation are reported. Talairach–Tourneaux (T-T) coordinates and ROI volume are provided for reference.
z-scores were computed to test the difference in strength of the correlations between wakefulness and sleep.
Correlation values within ROI reached $P < 0.001$ in all subjects ($n = 11$) and ROIs with the exception of two ROIs of one subject that were significant only to $P < 0.01$ (marked with #).
*Denotes significantly higher correlation ($P < 0.05$) during sleep compared to wakefulness.

Systemic Effects

An increase in BOLD fMRI fluctuation levels during light sleep in many cortical regions may be due, at least in part, to changes in perfusion unrelated to neuronal activity. Some studies have reported an increase in blood flow fluctuations after reduction in perfusion pressure [Fujii et al., 1990; Hudetz et al., 1992; Jones et al., 1995]. If sleep also reduces perfusion pressure, the possibly resultant blood flow fluctuations would be observable in the BOLD signal. However, this mechanism would not explain the fine scale, while widespread, spatial patterns of correlated activity seen during sleep, wakefulness [Fukunaga et al., 2006] and during visual fixation [Nir et al., 2006]. Nor does it explain the correlation observed between BOLD signal amplitude and EEG α power [Goldman et al., 2002; Laufs et al., 2006; Moosmann et al., 2003]. Simultaneous perfusion/BOLD fMRI studies might clarify this issue.

Alternative Origins of Resting State Activity During Sleep

Among the possible alternative explanations for the presence of resting state activity during sleep is the existence of dream-like reverie activity, which sometimes occurs during light sleep. Alternatively, or concurrently, it might also be that during sleep, fluctuations in the level of consciousness increase, and that they are reflected in local fluctuation in BOLD fMRI signal. For example, brief arousals could occur during light sleep that are too short to affect sleep score but nevetheless resulted in BOLD fMRI signal fluctuations. This is suggested by Laufs et al. [2006] findings and the current findings that IIoW correlates with BOLD fluctuation level in the visual cortex and other sensory areas (Fig. 3c). The correlation between BOLD fluctuation level in visual cortex and the EEG-derived IIoW suggests that BOLD fMRI could serve as a surrogate indicator of wakefulness when EEG is not available. Finally, it could be that the homeostatic processes that increase during sleep cause spatially distinct fluctuations in activity.

CONCLUSION

The continuation of resting-state BOLD fMRI signal fluctuations during sleep in several brain regions, including the hypothesized "default-mode network" of brain function suggests that this activity is not specific to the waking state. The fluctuation levels increase, particularly in primary sensory cortex, as the consciousness level decreases from wakefulness to light sleep. Further research is needed to establish a direct link between BOLD resting activity and electrical brain signals.

ACKNOWLEDGMENTS

The authors thank David A. Leopold (NIMH, NIH) for helpful suggestions.

REFERENCES

Allen PJ, Josephs O, Turner R (2000): A method for removing imaging artifact from continuous EEG recorded during functional MRI. Neuroimage 12:230–239.

Andersson JL, Onoe H, Hetta J, Lidstrom K, Valind S, Lilja A, Sundin A, Fasth KJ, Westerberg G, Broman JE, Watanabe Y, Langstrom B. (1998): Brain networks affected by synchronized sleep visualized by positron emission tomography. J Cereb Blood Flow Metab 18:701–715.

Arfanakis K, Cordes D, Haughton VM, Moritz CH, Quigley MA, Meyerand ME (2000): Combining independent component analysis and correlation analysis to probe interregional connectivity in fMRI task activation datasets. Magn Reson Imaging 18:921–930.

Arieli A, Sterkin A, Grinvald A, Aertsen A (1996): Dynamics of ongoing activity: Explanation of the large variability in evoked cortical responses. Science 273:1868–1871.

Bandettini PA, Wong EC, Hinks RS, Tikofsky RS, Hyde JS (1992): Time course EPI of human brain function during task activation. Magn Reson Med 25:390–397.

Berger H (1929): Über das Elektroenkephalogramm des Menschen. Archiv für Psychiatrie und Nervenkrankheiten 87:527–570.

Binder JR, Frost JA, Hammeke TA, Bellgowan PS, Rao SM, Cox RW (1999): Conceptual processing during the conscious resting state. A functional MRI study. J Cogn Neurosci 11:80–95.

Birn RM, Diamond JB, Smith MA, Bandettini PA (2006): Separating respiratory-variation-related fluctuations from neuronal-activity-related fluctuations in fMRI. Neuroimage 31:1536–1548.

Biswal B, Yetkin FZ, Haughton VM, Hyde JS (1995): Functional connectivity in the motor cortex of resting human brain using echo-planar MRI. Magn Reson Med 34:537–541.

Braun AR, Balkin TJ, Wesenten NJ, Carson RE, Varga M, Baldwin P, Selbie S, Belenky G, Herscovitch P (1997): Regional cerebral blood flow throughout the sleep-wake cycle. An H2(15)O PET study. Brain 120 (Part 7):1173–1197.

Buchsbaum MS, Mirsky AF, DeLisi LE, Morihisa J, Karson CN, Mendelson WB, King AC, Johnson J, Kessler R (1984): The Genain Quadruplets: Electrophysiological, positron emission, and X-ray tomographic studies. Psychiatry Res 13:95–108.

Bullmore ET, Suckling J, Overmeyer S, Rabe-Hesketh S, Taylor E, Brammer MJ (1999): Global, voxel, and cluster tests, by theory and permutation, for a difference between two groups of structural MR images of the brain. IEEE Trans Med Imaging 18:32–42.

Cordes D, Haughton VM, Arfanakis K, Wendt GJ, Turski PA, Moritz CH, Quigley MA, Meyerand ME (2000): Mapping functionally related regions of brain with functional connectivity MR imaging. AJNR Am J Neuroradiol 21:1636–1644.

Cordes D, Haughton VM, Arfanakis K, Carew JD, Turski PA, Moritz CH, Quigley MA, Meyerand ME (2001): Frequencies contributing to functional connectivity in the cerebral cortex in "resting-state" data. AJNR Am J Neuroradiol 22:1326–1333.

Creutzfeldt OD, Watanabe S, Lux HD (1966): Relations between EEG phenomena and potentials of single cortical cells. II. Spontaneous and convulsoid activity. Electroencephalogr Clin Neurophysiol 20:19–37.

De Luca M, Beckmann CF, De Stefano N, Matthews PM, Smith SM (2006): fMRI resting state networks define distinct modes of long-distance interactions in the human brain. NeuroImage 29:1359.

de Zwart JA, van Gelderen P, Kellman P, Duyn JH (2002): Application of sensitivity-encoded echo-planar imaging for blood oxygen level-dependent functional brain imaging. Magn Reson Med 48:1011–1020.

de Zwart JA, Ledden PJ, van Gelderen P, Bodurka J, Chu R, Duyn JH (2004): Signal-to-noise ratio and parallel imaging performance of a 16-channel receive-only brain coil array at 3.0 Tesla. Magn Reson Med 51:22–26.

Drummond SP, Bischoff-Grethe A, Dinges DF, Ayalon L, Mednick SC, Meloy MJ (2005): The neural basis of the psychomotor vigilance task. Sleep 28:1059–1068.

Evarts EV, Bental E, Bihari B, Huttenlocher PR (1962): Spontaneous discharge of single neurons during sleep and waking. Science 135:726–728.

Fox PT, Mintun MA (1989): Noninvasive functional brain mapping by change-distribution analysis of averaged PET images of H215O tissue activity. J Nucl Med 30:141–149.

Fransson P (2006): How default is the default mode of brain function? Further evidence from intrinsic BOLD signal fluctuations. Neuropsychologia 44:2836–2845.

Fujii K, Heistad DD, Faraci F (1990): Vasomotion of basilar arteries in vivo. Am J Physiol Heart Circ Physiol 258:1829.

Fukunaga M, Horovitz SG, van Gelderen P, de Zwart JA, Jansma JM, Ikonomidou VN, Chu R, Deckers RHR, Leopold DA, Duyn JH (2006): Large-amplitude, spatially correlated fluctuations in BOLD fMRI signals during extended rest and early sleep stages. Magn Reson Imaging 24:979–992.

Goldman RI, Stern JM, Engel J Jr, Cohen MS (2002): Simultaneous EEG and fMRI of the alpha rhythm. Neuroreport 13:2487–2492.

Greicius MD, Krasnow B, Reiss AL, Menon V (2003): Functional connectivity in the resting brain: A network analysis of the default mode hypothesis. Proc Natl Acad Sci USA 100:253–258.

Gusnard DA, Raichle ME (2001): Searching for a baseline: Functional imaging and the resting human brain. Nat Rev Neurosci 2:685–694.

Hampson M, Peterson BS, Skudlarski P, Gatenby JC, Gore JC (2002): Detection of functional connectivity using temporal correlations in MR images. Hum Brain Mapp 15:247–262.

Hofle N, Paus T, Reutens D, Fiset P, Gotman J, Evans AC, Jones BE (1997): Regional cerebral blood flow changes as a function of delta and spindle activity during slow wave sleep in humans. J Neurosci 17:4800–4808.

Holmes AP, Blair RC, Watson G, Ford I (1996): Nonparametric analysis of statistic images from functional mapping experiments. J Cereb Blood Flow Metab 16:7.

Howell DC (1997): Statistical Methods for Psychology. Belmont, CA: Wadworth Publishing. 724 p.

Hudetz AG, Roman RJ, Harder DR (1992): Spontaneous flow oscillations in the cerebral cortex during acute changes in mean arterial pressure. J Cereb Blood Flow Metab 12:491–499.

Jones CJH, Kuo L, Davis MJ, Chilian WM (1995): Regulation of coronary blood flow: Coordination of heterogeneous control mechanisms in vascular microdomains. Cardiovasc Res 29:585–596.

Kajimura N, Uchiyama M, Takayama Y, Uchida S, Uema T, Kato M, Sekimoto M, Watanabe T, Nakajima T, Horikoshi S, et al. (1999): Activity of midbrain reticular formation and neocortex during the progression of human non-rapid eye movement sleep. J Neurosci 19:10065–10073.

Kajimura N, Nishikawa M, Uchiyama M, Kato M, Watanabe T, Nakajima T, Hori T, Nakabayashi T, Sekimoto M, Ogawa K, et al. (2004): Deactivation by benzodiazepine of the basal forebrain and amygdala in normal humans during sleep: A placebo-controlled [15O]H2O PET study. Am J Psychiatry 161: 748–751.

Kiviniemi VJ, Haanpaa H, Kantola JH, Jauhiainen J, Vainionpaa V, Alahuhta S, Tervonen O (2005): Midazolam sedation increases fluctuation and synchrony of the resting brain BOLD signal. Magn Reson Imaging 23:531–537.

Kjaer TW, Law I, Wiltschiotz G, Paulson OB, Madsen PL (2002): Regional cerebral blood flow during light sleep–a H(2)(15)O-PET study. J Sleep Res 11:201–207.

Kwong KK, Belliveau JW, Chesler DA, Goldberg IE, Weisskoff RM, Poncelet BP, Kennedy DN, Hoppel BE, Cohen MS, Turner R, et al. (1992): Dynamic magnetic resonance imaging of human brain activity during primary sensory stimulation. Proc Natl Acad Sci USA 89:5675–5679.

Laufs H, Kleinschmidt A, Beyerle A, Eger E, Salek-Haddadi A, Preibisch C, Krakow K (2003): EEG-correlated fMRI of human alpha activity. Neuroimage 19:1463–1476.

Laufs H, Holt JL, Elfont R, Krams M, Paul JS, Krakow K, Kleinschmidt A (2006): Where the BOLD signal goes when alpha EEG leaves. Neuroimage 31:1408–1418.

Laureys S (2005): The neural correlate of (un)awareness: Lessons from the vegetative state. Trends Cogn Sci 9:556–559.

Leopold DA, Murayama Y, Logothetis NK (2003): Very slow activity fluctuations in monkey visual cortex: Implications for functional brain imaging. Cereb Cortex 13:422–433.

Lowe MJ, Mock BJ, Sorenson JA (1998): Functional connectivity in single and multislice echoplanar imaging using resting-state fluctuations. Neuroimage 7:119–132.

Lowe MJ, Dzemidzic M, Lurito JT, Mathews VP, Phillips MD (2000): Correlations in low-frequency BOLD fluctuations reflect cortico-cortical connections. Neuroimage 12:582–587.

Lund TE, Madsen KH, Sidaros K, Luo WL, Nichols TE (2006): Non-white noise in fMRI: Does modelling have an impact? Neuroimage 29:54–66.

Maquet P (2000): Functional neuroimaging of normal human sleep by positron emission tomography. J Sleep Res 9:207–231.

Maquet P, Dive D, Salmon E, Sadzot B, Franco G, Poirrier R, Franck G (1992): Cerebral glucose utilization during stage 2 sleep in man. Brain Res 571:149–153.

Mazoyer B, Zago L, Mellet E, Bricogne S, Etard O, Houde O, Crivello F, Joliot M, Petit L, Tzourio-Mazoyer N (2001): Cortical networks for working memory and executive functions sustain the conscious resting state in man. Brain Res Bull 54:287–298.

McGuire PK, Paulesu E, Frackowiak RS, Frith CD (1996): Brain activity during stimulus independent thought. Neuroreport 7:2095–2099.

Mintun MA, Raichle ME, Martin WR, Herscovitch P (1984): Brain oxygen utilization measured with O-15 radiotracers and positron emission tomography. J Nucl Med 25:177–187.

Mitra PP, Ogawa S, Hu X, Ugurbil K (1997): The nature of spatiotemporal changes in cerebral hemodynamics as manifested in functional magnetic resonance imaging. Magn Reson Med 37:511–518.

Moosmann M, Ritter P, Krastel I, Brink A, Thees S, Blankenburg F, Taskin B, Obrig H, Villringer A (2003): Correlates of alpha rhythm in functional magnetic resonance imaging and near infrared spectroscopy. Neuroimage 20:145–158.

Moruzzi G, Magoun HW (1995): Brain stem reticular formation and activation of the EEG. 1949. J Neuropsychiatry Clin Neurosci 7:251–267.

Nir Y, Hasson U, Levy I, Yeshurun Y, Malach R (2006): Widespread functional connectivity and fMRI fluctuations in human visual cortex in the absence of visual stimulation. Neuroimage 30:1313–1324.

Nofzinger EA, Buysse DJ, Miewald JM, Meltzer CC, Price JC, Sembrat RC, Ombao H, Reynolds CF, Monk TH, Hall M, et al. (2002): Human regional cerebral glucose metabolism during non-rapid eye movement sleep in relation to waking. Brain 125 (Part 5):1105–1115.

Obrig H, Neufang M, Wenzel R, Kohl M, Steinbrink J, Einhaupl K, Villringer A (2000): Spontaneous low frequency oscillations of cerebral hemodynamics and metabolism in human adults. Neuroimage 12:623–639.

Ogawa S, Lee TM, Kay AR, Tank DW (1990): Brain magnetic resonance imaging with contrast dependent on blood oxygenation. Proc Natl Acad Sci USA 87:9868–9872.

Peigneux P, Laureys S, Delbeuck X, Maquet P (2001): Sleeping brain, learning brain. The role of sleep for memory systems. Neuroreport 12:A111–A124.

Raichle ME (2006): Neuroscience. The brain's dark energy. Science 314:1249–1250.

Raichle ME, MacLeod AM, Snyder AZ, Powers WJ, Gusnard DA, Shulman GL (2001): A default mode of brain function. Proc Natl Acad Sci USA 98:676–682.

Rechtschaffen A,Kales A, editors (1968): A Manual of Standarized Terminology, Techniques and Scoring System for Sleep Stage of Human Subjects. Bethesda, MD: U.S. Department of Health, Education and Welfare. Public Health Service. National Institutes of Health, NINDS.

Saad ZS, Chen G, Reynolds RC, Christidis PP, Hammett KR, Bellgowan PS, Cox RW (2006): Functional imaging analysis contest (FIAC) analysis according to AFNI and SUMA. Hum Brain Mapp 27:417–424.

Sadato N, Pascual-Leone A, Grafman J, Ibanez V, Deiber MP, Dold G, Hallett M (1996): Activation of the primary visual cortex by Braille reading in blind subjects. Nature 380:526–528.

Sadato N, Nakamura S, Oohashi T, Nishina E, Fuwamoto Y, Waki A, Yonekura Y (1998): Neural networks for generation and suppression of alpha rhythm: A PET study. Neuroreport 9:893–897.

Shulman GL, Corbetta M, Buckner RL, Fiez JA, Miezin FM, Raichle ME, Petersen SE (1997a): Common blood flow changes across visual tasks. I. Increases in subcortical structures and cerebellum but not in nonvisual cortex. J Cogn Neurosci 9:624–647.

Shulman GL, Fiez JA, Corbetta M, Buckner RL, Miezin FM, Raichle ME, Petersen SE (1997b): Common blood flow changes across visual tasks. II. Decreases in cerebral cortex. J Cogn Neurosci 9:648–663.

Tzourio-Mazoyer N, Landeau B, Papathanassiou D, Crivello F, Etard O, Delcroix N, Mazoyer B, Joliot M (2002): Automated anatomical labeling of activations in SPM using a macroscopic anatomical parcellation of the MNI MRI single-subject brain. Neuroimage 15:273–289.

van de Ven VG, Formisano E, Prvulovic D, Roeder CH, Linden DE (2004): Functional connectivity as revealed by spatial independent component analysis of fMRI measurements during rest. Hum Brain Mapp 22:165–178.

Wise RG, Ide K, Poulin MJ, Tracey I (2004): Resting fluctuations in arterial carbon dioxide induce significant low frequency variations in BOLD signal. Neuroimage 21:1652–1664.

Zeman A (2001): Consciousness. Brain 124 (Part 7):1263–1289.